IS-PORTO 2023 PROCEEDINGS

Proceedings of the 8th International Symposium on DEFORMATION CHARACTERISTICS OF GEOMATERIALS Porto, 3rd - 6th September 2023

Liquefaction behaviour of aluminium and plastic rod assemblies using bi-axial apparatus with application of image analysis

Rawiwan Sukhumkitcharoen[1], *Junichi* Koseki[1], *Hiroyuki* Kyokawa[2] and *Masahide* Otsubo[3]

[1]*The University of Tokyo, Department of Civil Engineering, 7-3-1 Hongo, Bunkyo-ku, Tokyo, Japan*
[2]*Nagoya Institute of Technology, Gokiso-cho, Nagoya, Aichi, 466-8555, Japan*
[3]*Public Works Research Institute, 1-6 Minamihara, Tsukuba, Ibaraki, 305-8516, Japan*
[#]*Corresponding author: Sukhumkitcharoen-rawiwan@g.ecc.u-tokyo.ac.jp*

ABSTRACT

It has recently been shown that the overall deformation characteristics of granular materials during liquefaction seems to be governed by local void ratio characteristics. The aim of this study is to investigate the relationship between mechanical properties and local void ratio changes during liquefaction in two materials of different weights (aluminium-type and plastic-type rod assemblies). A series of constant-volume cyclic bi-axial loading tests was conducted together with the image analysis obtaining local void behaviour. The experimental results demonstrate that the first liquefaction resistance of the plastic sample is higher than the aluminium one, corresponding to its smaller initial void ratio and less contractive behaviour observed in the early stage of drained monotonic compression. However, after experiencing the first liquefaction and subsequent re-consolidation histories, a liquefiable assembly of aluminium and plastic rods both became either denser (densification) or more homogenous (homogenization) in terms of local void ratio, suggesting an increase in liquefaction resistance in the next liquefaction stage. This work also includes a preliminary analogous study using a semi-3D discrete element method (DEM) with one single layer of spherical particles to simulate the similar liquefaction behaviour observed in the laboratory tests.

Keywords: Liquefaction; local void ratio; bi-axial test; discrete element method.

1. Introduction

Liquefaction has been considered as one of severe natural disasters after causing extensive damages to infrastructures, buildings, and human life (Towhata 2008). Unfortunately, based on the complexity of the liquefaction mechanism, the general question regarding the performance of densified-soil deposit ground against liquefaction is still doubted and cannot be clearly answered. Therefore, a comprehensive knowledge of liquefaction behaviour is prerequisite for effective assessment of liquefaction potential.

The evidence showing that the susceptibility of soil can sway regardless of density was revealed and confirmed piece by piece in both field case studies and laboratory tests. For example, unpredictable liquefaction resistance was pointed out in 2011 Tohoku Earthquake event (Wakamatsu 2012), and also along the transient stages in the 1-g shaking table test using fine and clean sand (Teparaksa and Koseki 2018) despite densification. Furthermore, Seed et al. (1977) found an increase of liquefaction resistance with no change in relative density. With the above peculiar observations, the awareness of microscopic evaluation in liquefaction study (Wahyudi et al. 2014; Morimoto et al. 2021) has been raised again to seek for other key factors behind these phenomena.

Since the mid-20th century, the significant influence of the local void ratio, which is a void ratio in a specified area, in terms of its average and standard deviation values on the engineering properties of soil has been recognized (Mogami 1965). It is noteworthy that local void ratio by plotting in spatial distribution is more relevant to the microstructure or fabric of the sample rather than trivial factors like its density or global void ratio. Afterward, a considerable effort was made to evaluate the local void ratio of granular samples employing various approaches on a wide range of topics (Oda et al. 1985; Konishi and Naruse 1988; Al-Raoush and Alshibli 2006), yet a limited number of researchers (e.g. Koseki et al. 2020) has focused on the study of liquefaction behaviour utilizing microscopic investigation, especially in the aspect of local void ratio characteristics.

As a continuation of Koseki's study, this study conducted a series of replicating cyclic bi-axial tests on the assembly of rods under constant-volume condition, introducing two different types of materials: aluminium and plastic rods. Plastic rod has been rarely used in the literature, but it was employed in this study for the purpose of verification and comparison of liquefaction behaviour between heavier and lighter materials. Differences in liquefaction resistance are examined along with their basic mechanical behaviours observed in drained compression tests. With the application of the image analysis approach, the change of the local void ratio observed in the two materials during liquefaction stage is further visualized and discussed. In order to

unveil a legitimate and profound liquefaction mechanism for these materials, experimental results observed in both cases were also simulated using the discrete element method (DEM). By mimicking these experimental tests, a preliminary comparision is made on the liquefaction characteristics observed between the bi-axial tests and DEM models.

2. Experimental setup

2.1. Materials

In this study, two types of granular materials of different weights (aluminium and plastic) were used, which are in the shape of a 50mm-long circular rod, as shown in Figs. 1(a) and 1(b), respectively. The aluminium rods have a specific gravity of 2.685, consisting of two different diameter sizes, 3.0 mm and 1.6 mm (to be denoted as thick and thin rods, respectively). While the plastic rods made from polystyrene with the lower specific gravity of 1.019 have the same geometric dimension aside from the cross-section of the thin rod being 2.0 mm.

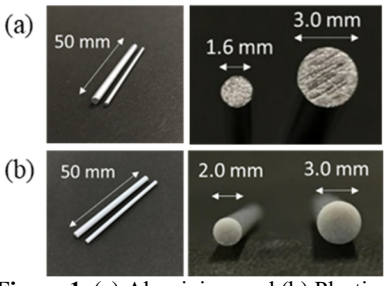

Figure 1. (a) Aluminium rod (b) Plastic rod.

2.2. Apparatus

Bi-axial apparatus and its schematic drawing are demonstrated in Figs. 2(a) and 2(b). This device can perform stress-controlled (consolidation) and strain-controlled systems (for example, monotonic shearing and cyclic loading) by controlling pneumatic cylinders and motor-driven screw jacks, respectively. The measurements of stress and strain in vertical and horizontal directions were done by using three loadcells (CH0, CH1 and CH2) and three external displacement transducers (EDT-1, EDT-2 and EDT-3) attached on wall frames. As can be seen in the upper-left side of Fig. 2(a), a digital camera with a resolution of 7360×4912 pixels and an LED ring-light were set in the front of the specimen in order to track the change of local void ratio.

2.3. Test procedure

2.3.1. Liquefaction test

The overall cyclic loading test process can be divided into five stages, which are sample preparation, consolidation, liquefaction, re-consolidation, and second liquefaction. It should be noted that this paper mainly discusses on the results up to the re-consolidation stage. In this paper, the result of second liquefaction stage is mentioned roughly about the changes in liquefaction resistance influenced by the former stages.

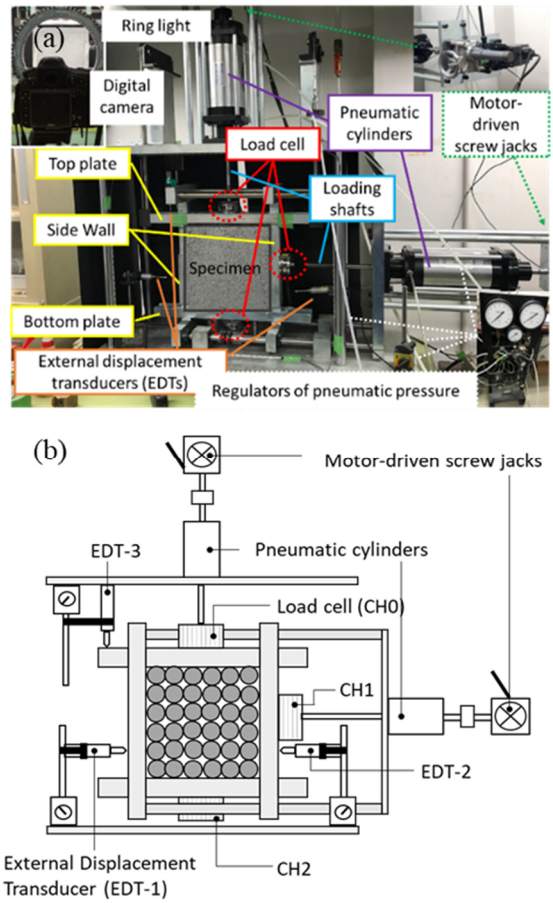

Figure 2. (a) Bi-axial apparatus (b) Schematic drawing of bi-axial apparatus.

During sample preparation, two sizes of rods were stacked into the wall frame by hand and mingled with a mixing ratio of thick to thin rods as 1 to 6 by number (or 3 to 5 by weight) for aluminium rod case and 2 to 3 by weight for plastic rod case. The purpose of this stage is to prepare the samples in which their dimensions are in the range of 266-273 mm in height and 300-305 mm in width. As a result, the variation of the initial void ratio of the specimen is in-between 0.221 to 0.231 for the aluminium case and 0.200 to 0.218 for the plastic rod case.

Then, the specimens were subjected to isotropic compression at 100 kPa during the consolidation stage. The following application of 30 kPa and 60 kPa deviator cyclic loading under a constant-volume condition in the case of aluminium and plastic, respectively, is called liquefaction stage. It should be noted that the cyclic loadings were exerted under a constant strain rate of 0.0081 mm/sec until the double amplitude vertical strain ($\varepsilon_{DA,V}$) reached 2%. In this study, the definition of liquefaction is based on this target strain. The liquefaction process of saturated soil, namely the build-up of pore water pressure during cyclic loading under undrained condition, can be simulated as the reduction of mean stress in dry rod assemblies while biaxial cyclic loading with maintaining a constant volume. These procedures under the same conditions were repeated in the re-consolidation and second liquefaction stages.

Aside from the above cyclic loading tests, the deep investigation of monotonic behaviour was also done by

conducting four cases of Consolidated-Drained tests (CD tests) under different constant horizontal stress, 10, 20, 30, and 60 kPa. The testing program for two types of materials is summarized in Table 1.

Table 1. Testing program

Testing conditions	Consolidated-Drained tests (CD tests)	Liquefaction tests
Type	Monotonic loading	Cyclic loading
Controlling system	Drained	Constant volume
Number of tests	4 for each rod type	1 for Al, 2 for Plastic
Variable	Constant horizontal stress	CSR
Cases	10,20,30, 60 kPa	0.15, 0.3

2.3.2. Image analysis: Evaluation of local void ratio

As typically shown in Fig. 3, there are three substages of the image analysis procedure: image processing, calculation of local void ratio, and formation of void ratio mesh. Firstly, the original RGB image was converted into a grayscale image and binary image in order. The segmentation, which is the process of distinguishing the void parts that are much darker than the rod parts in a grayscale image, is quite sensitive by using a single threshold value. Then, the trial on proper threshold value by calibrating with global void ratio calculated by the weighing method is implemented to encourage the validation of local void ratio.

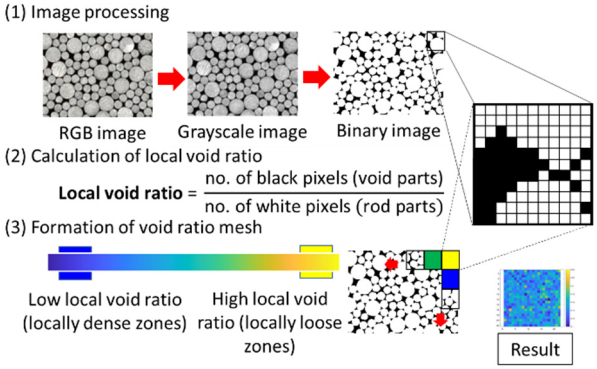

Figure 3. Schematic figure showing image analysis procedures.

When a good-quality binary image (all of the rod parts be turned to white color and all of the void parts be changed to black color) was achieved, the study area of 200 mm×200 mm at the central part of the specimen was divided into smaller 10-mm square grid in order to evaluate local void ratio (e_{ij}) in terms of the ratio of a number of black pixels to a number of white pixels. Each grid will be occupied by its local void ratio, representing with the color scheme from blue to yellow as locally dense zone ($low\ e_{ij}$) to locally loose zones ($high\ e_{ij}$), which can be called as void ratio mesh.

3. Physical liquefaction behaviour

3.1. Basic information of rod assemblies

The basic characteristics of two types of rod assemblies could be simply investigated by conducting CD tests. Fig. 4(a) shows eight typical stress-strain relationships of aluminium (denoted by black lines) and plastic (denoted by red lines) samples at four constant horizontal confining stress. As can be seen, by considering vertical strain up to 2%, all black lines seem to lie a bit below red lines before reaching similar stress states. It may be implied that aluminium samples exhibited slightly softer behaviour, corresponding to higher initial void ratio.

Relationships between volumetric strain and vertical strain of two materials are shown in Fig. 4(b). At a small strain level ($\varepsilon_v < 2\%$), plastic samples show less contractive behaviour (positive sign means being contracted) at all different confining stages, which is consistent with their stress-strain behaviour. The overall monotonic properties suggest that the aluminium sample might be more prone to liquefaction than the plastic sample. It should be acknowledged that their initial conditions and mechanical behaviour are based on the adopted sample preparation method.

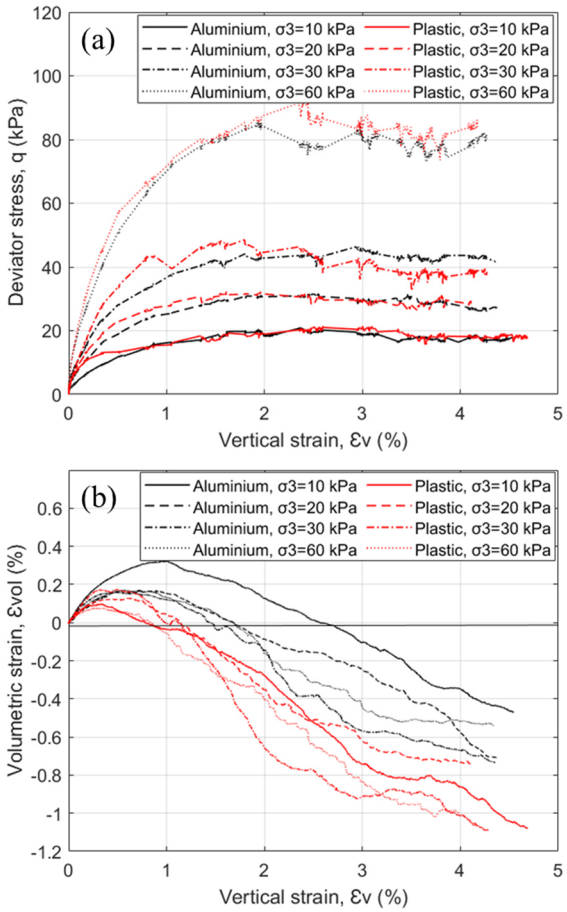

Figure 4. CD testing's results (a) stress-strain relationship (b) volume change characteristic in CD tests.

3.2. Liquefaction behaviour of rod assemblies

Stress-strain relationships in the first liquefaction stage between two types of materials are compared in

Fig. 5. Under the same confining stress state at 100 kPa, the first liquefaction resistance, which is quantified by the number of loading cycles when the test was terminated, is higher in case of plastic rod. As can be seen, the plastic sample with the application of deviator stress at CSR=0.15 (q_{cyclic} = 30 kPa) could not develop enough strain to induce liquefaction. While the $\varepsilon_{DA,V}$ of the aluminium one was easily accumulated as the cyclic loadings have been applied. It can be implied that plastic sample is stronger than aluminium sample against liquefaction.

In order to study the change of local void ratio during liquefaction, the deviator stress during cyclic loading had to be increased from 30 kPa to 60 kPa (CSR = 0.30) to stimulate the liquefied plastic sample. The latter case of plastic sample will be discussed along with the aluminium case in the next section.

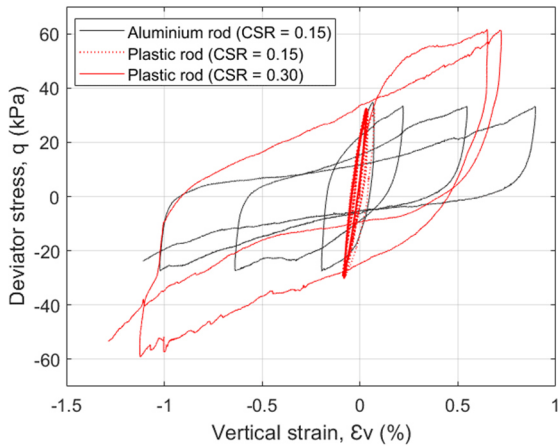

Figure 5. Stress-strain relationship in the first liquefaction stage.

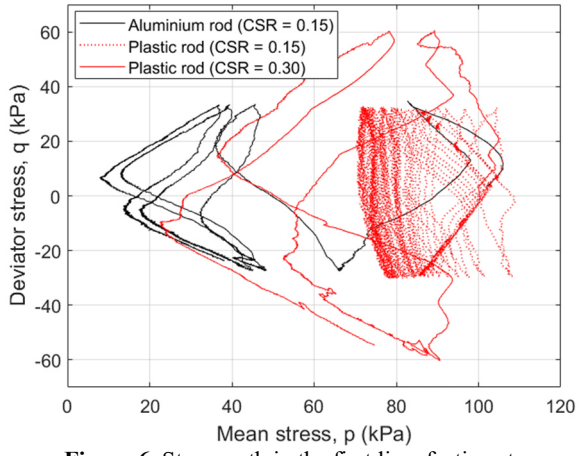

Figure 6. Stress path in the first liquefaction stage.

Their stress paths are also presented in Fig. 6. As the samples have been subjected to cyclic loadings, the different reduction rate of mean stress per cycle was distinguished, corresponding to their strain development explained earlier. When comparing a plastic sample with a CSR of 0.15 to an aluminium sample, it is obvious that shearing the plastic sample did not cause a significant reduction in volume (negative dilatancy), which would have led to substantial swelling without any increase in volume. As a result, the mean stress was reduced by a relatively small amount. It could be confirmed that the extent of negative dilatancy became significant, and the plastic sample was prone to liquefaction similarly to aluminium sample when CSR increased to 0.30.

The results of CD tests emphasize that volume change characteristics may be the main reason to induce such behaviour in this time. As a well-known correlation between the volume changes during drained shearing and pore water pressure change during typical undrained shearing, it confirms that the contractive behaviour may dominantly affect the response of specimen during the first quarter cycle of cyclic loading, suggesting less reduction of mean stress and more difficulty to liquefy. These observations further support the importance of a deeper study on the influence of the local void ratio, which governs the overall dilatancy of the specimen.

4. Statistical behaviour of local void ratio

The change of local void ratio can be tracked and analyzed in a statistical manner by plotting the spatial distributions of local void ratio (called as void ratio mesh) as shown in Fig. 7 and their frequency distributions at the intermediate stages starting from before/after liquefaction to after re-consolidation are summarized in Figs. 8(a) and 8(b), respectively, for aluminium and plastic cases. By considering the tendency of particle rearrangement due to the action of cyclic loading denoted with blue-solid line (Before 1st Liq.) and blue-dotted line (After 1st Liq.), homogenization is performed with the reduction of coefficient of variation (C.V.) in both cases. As can be seen in graphical representations, the peak at the specified local void ratio was shifted to a higher position, introducing a more common in terms of local void ratio in aluminium case. In comparison, a plastic sample with a lower average local void ratio showed different behaviour, yet the same trend in which the elimination of locally relatively dense and loose zones was observed. It should be noted that the attempt for redistribution of particles under constant-volume condition can cause a small increment of the average local void ratio within the study area, which is not considered the whole part of the specimen.

In the same figures, the local void ratio distributions after re-consolidation are also represented using the orange-solid lines. The densification inside the specimen was manifested with the evidence of a smaller average local void ratio in both cases. Furthermore, it can clearly be seen that the graphs tend to shift to the left side (denser zone with a lower local void ratio), especially in the plastic case. For the less change of average local void ratio in aluminium rod case, the increase of the ratio of locally dense zones to locally loose zones is still detected.

From the above observations, the homogenization and densification could be validated as an overall change at each stage. In order to investigate the response of particles in an individual grid throughout all loading histories, the spatial distributions of local void ratio increments induced by liquefaction and subsequent re-consolidation histories (LR histories) are further plotted in Fig. 9(a) for the aluminium case and Fig. 9(b) for the plastic case. The initial local void ratio at the start of the liquefaction stage (ei) is plotted against the increment of

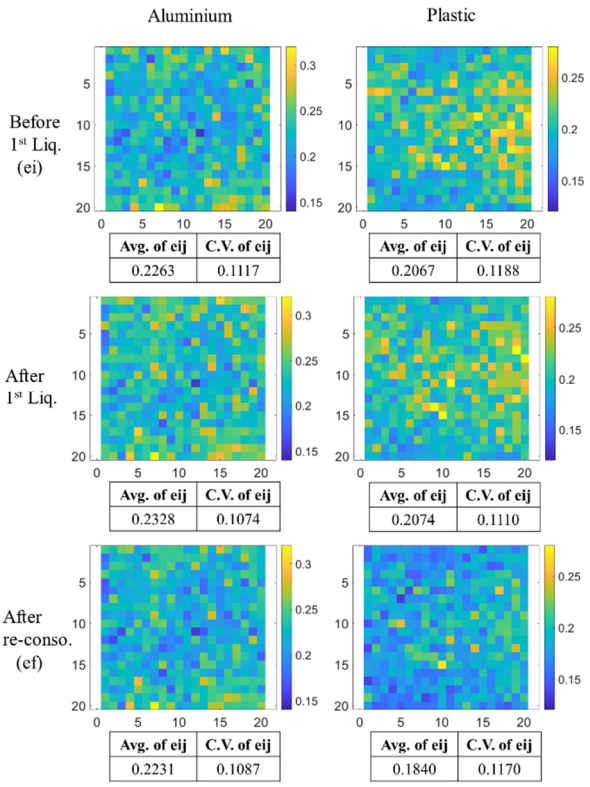

Figure 7. Void ratio mesh at several stages.

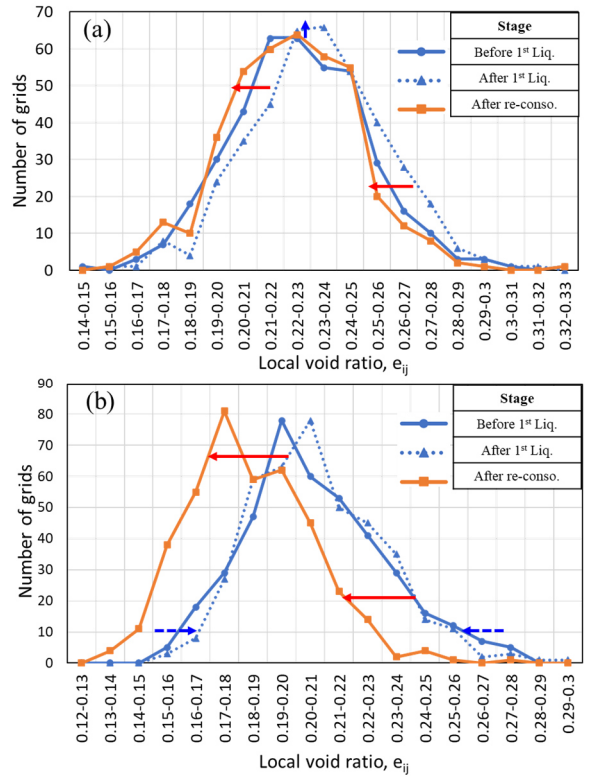

Figure 8. Frequency distribution of the local void ratio of (a) aluminium rod sample (b) plastic rod sample.

the local void ratio caused by LR histories (Δe_{ij}= ef-ei, when ef is the local void ratio after the re-consolidation stage). The negative linear regression observed in two cases is another piece of evidence supporting the reformation of a homogenous specimen. As pointed out in Fig. 8(a), the particles in initially relatively loose zones tended to become denser, while in initially relatively dense zones tended to become looser. This behaviour, which shows the dislocation of particles to a more uniform state, is indeed consistent with the previous research conducted by Koseki et al. (2020). The barely immense assemblage of points on the negative side is also compatible with overall densification.

As mentioned earlier, the subsequent compression of plastic sample is quite tremendous in all areas, resulting in a comparatively huge amount of reduction in the average local void ratio. Instead of slightly loosening in initially locally dense zones, less intensity of densification was performed in the case of plastic rods.

As a result of overall densification and homogenization, the samples were less vulnerable to liquefaction, which requires a larger number of cycles to liquefy; 10 times and 6 times, respectively, for aluminium and plastic samples, in the following liquefaction stages. It could be inferred that new structures induced by the LR histories can enhance the liquefaction resistance in any type of material.

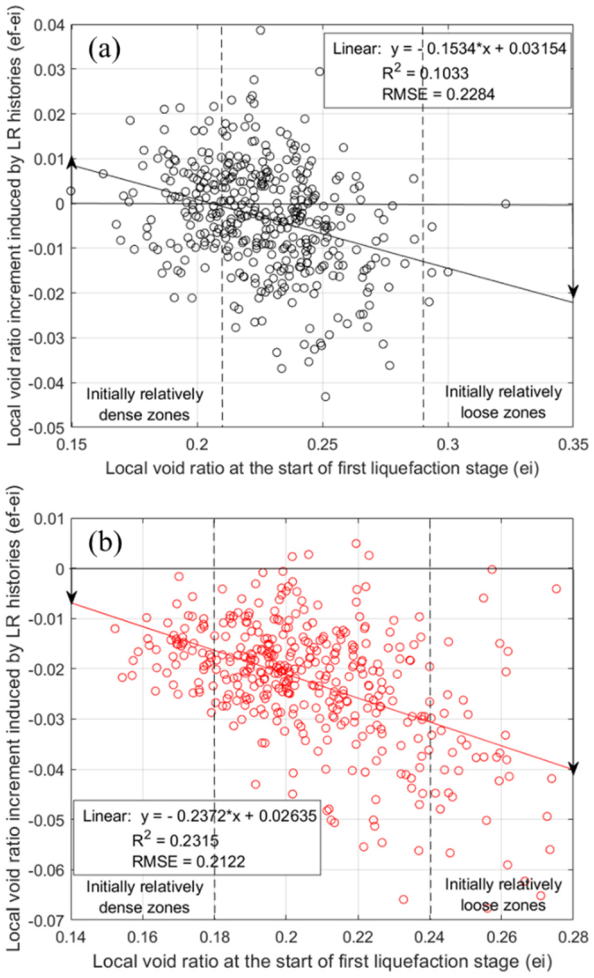

Figure 9. Spatial distribution of the local void ratio of (a) aluminium rod sample (b) plastic rod sample.

5. Liquefaction simulation using DEM

5.1. Simulation method

The discrete element method (DEM) is one of the most effective and powerful numerical tools to simulate equivalent experimental studies based on particle

interaction (Cundall and Strack 1979). The DEM model may enhance quantifying some challenging parameters that are difficult to be directly measured in the laboratory, such as soil fabrics, however, its validation can be questioned sometimes. In this study, some implementations on a modified version of LAMMPS (Large-scale Atomic/Molecular Massively Parallel Simulator) (Plimpton 1995), as well as the physical measurement of some material properties, were employed to replicate similar environments to bi-axial testing in the laboratory as close as possible.

The benchmark simulations of these liquefaction tests were performed using the simplified Hertz-Mindlin contact model, which has been widely adopted (Hertz 1882; Mindlin 1949; Morimoto et al. 2021). For simplicity and high efficiency of computation time, a single layer of spherical particles confined by rigid boundaries was generated, which can be called as a semi-3D DEM model (Adesina et al. 2022). By doing so, there are three concerns for simulating a planar or 2D environment in a 3D scale; mass (m), the moment of inertia (I), and stress (σ) calculation. In such a case, the calibration factor was assigned to actual particle density to keep the single-particle sphere's mass the same as the rod's. The stress calculation is also based on wall stress, which was confirmed to be equivalent with the particle's mean stress. In this study, only the moment of inertia was considered less sensitive to the overall results under a small difference between I_{rod} and I_{sphere}.

In order to distinguish liquefaction behaviour between two materials and calibrate the DEM model, some physical properties of particles assigned in the current model were directly measured. For example, density from mass-and-volume measurement, particle shear modulus from single particle compression test, and inter-particle friction coefficient from inclined slope test. Simulation conditions and parameters used in this study are summarized in Table 2.

Similar to the laboratory testing, analogous processes under the same testing conditions, including the image analysis part, are illustrated in Fig. 10. However, there are two sub-stages during the sample preparation process in DEM; pluviation (step 1) and top-wall generation (step 2), which is a different strategy from typical sample preparation methods in DEM such as particle expansion method (e.g., Xie and Zhao, 2022) in order to include the effect of gravity. By controlling viscous damping and local damping in these stages, the looser aluminium sample (with e = 0.210) and denser plastic sample (with e = 0.191) were achieved. Similar testing conditions were also repeated in consolidation (step 3) and liquefaction stages (step 4). For keeping the volume constant during cyclic loading, the absolute lateral velocity of two side walls (v_l) was registered as the function of the absolute vertical velocity of the upper-and-bottom wall (v_h) and updated specimen's dimension both length (L) and height (H) in the entire process, as expresssed in Eq. (1).

$$v_l = -\frac{L}{H} v_h \quad (1)$$

It should be noted that image analysis for evaluating local void ratio can be proceeded on the DEM side by updating the position of each particle and plotting in a cartesian coordinate system. The pre-processing from the X-Y coordinate scale to the pixel scale will be followed by similar processes explained before. In the next section, only some parts of the results from the model's calibration and validation process will be discussed at the outset of the DEM study.

Table 2. DEM parameters used in the study

Sample	Aluminium	Plastic	Wall
Number of particles	23985	16810	
Density (kg/m^3)	2685	1019	
Shear modulus (GPa)	28	7.35	80
Poisson's ratio	0.33	0.35	0.3
Friction coefficient	0.4	0.255	Same as particle
Void ratio (before shearing)	0.210	0.191	
Viscous damping coefficient	0 0.1 (step 2)	0 (all)	
Local damping coefficient	0 0.5 (step 1)	0 (all)	
Particle size distribution	Same as experiments		

*Step is defined in Fig. 10

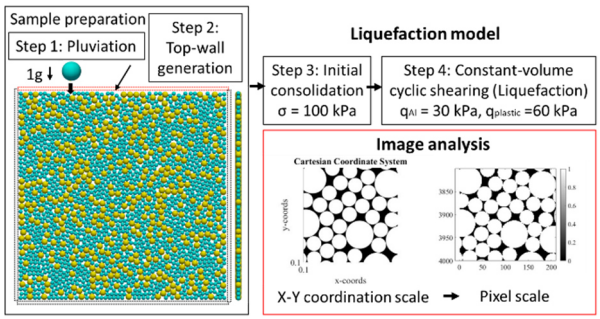

Figure 10. Schematic diagram of simulation procedures.

5.2. Simulation results

When the attempts to mimic the laboratory testing have been adopted, the liquefaction behaviours observed in both experimental study and numerical simulation can be revealed in Fig. 11, in which the stress-strain relationship and stress path of aluminium sample and plastic sample are shown accordingly. It can be observed from stress-strain relationships that the softening was performed as cyclic loading applied until termination, potentially in aluminium sample, which is consistent with the laboratory result. It could also be confirmed that the first liquefaction resistance of plastic sample under current conditions is higher than aluminium one. A more resilient sample against liquefaction that requires larger CSR to arouse its liquefied stage was also discovered in the denser sample in the DEM study performed by Otsubo and et al. (2022).

Herein, the influence of swelling behaviour on the residual mean effective stress, which is a minimum value of remaining mean stress in the last loading cycle, is discussed. It is interesting that the residual effective mean

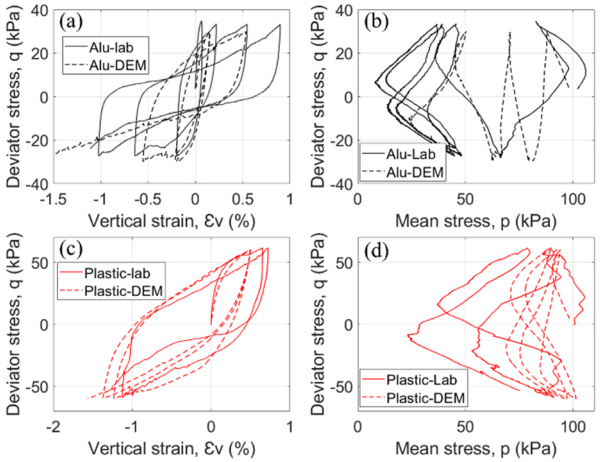

Figure 11. Comparison between laboratory test result and DEM result (a) stress-stain of aluminium (b) stress path of aluminium (c) stress-stain of plastic (d) stress path of plastic.

stress of four lines in Figs. 11(b) and 11(d), corresponds to the unloading behaviour illustrated in Fig. 12. This figure explains the relationship between volumetric strain and relative mean stress (in terms of the ratio of current stress to initial stress). When the confining stress of 100 kPa was released, the mean stress of the softer material (with a steeper slope) will remain higher than the stiffer one at the same volumetric strain changes, suggesting the same order in residual mean stress. It may be inferred that swelling characteristics in bi-axial tests and DEM simulations have a good agreement with liquefaction behaviour that can be used as one of information for rough screen liquefaction behaviours when considering different types of materials. Still, there is a room for improvement in this current model's performance for a better understanding of liquefaction behaviour.

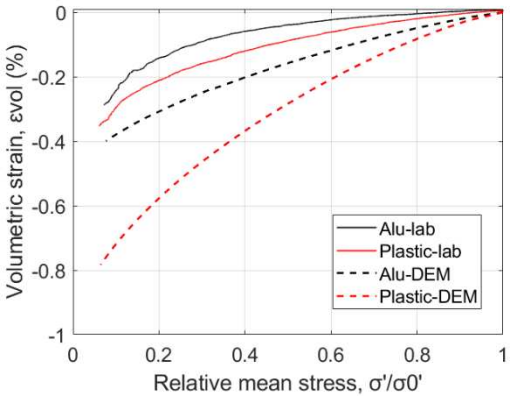

Figure 12. Unloading behaviour of aluminium and plastic rod samples observed in laboratory and DEM.

6. Conclusions

The importance of local void ratio on liquefaction study has been confirmed throughout observations in this study. First of all, the first liquefaction resistance is higher in plastic rod case due to its structural arrangement produced by current preparation method. It suggests that the smaller initial void ratio with less contractive behaviour, which is the global response of plastic sample influenced by distribution of local void ratio, seems to be predominant on liquefaction behaviour. Furthermore, by considering the change of local void ratio caused by liquefaction and following re-consolidation histories, there are two main characteristics observed in both types of materials, densification and homogenization.

1. Densification: the overall reduction of local void ratio (Smaller average local void ratio, the overall shift of local void ratio distribution to the denser side)
2. Homogenization: the reduction of non-uniformity of local void ratio distribution (Smaller C.V. value, narrower range of local void ratio, profound densification in locally loose zones)

These observations provide further support on the strengthening effect in which rearrangements of particles, not only densification but also homogenization, would have a positive effect on the increase of liquefaction resistance in the upcoming liquefaction stages.

As a brief introduction in the last section, the differences between two materials could also be distinguished in DEM simulation. Moreover, the relationship between monotonic unloading behaviour and liquefaction behaviour was confirmed, suggesting less residual mean stress in stiffer material under the same volumetric strain. The current version of DEM simulation requires additional improvements for reproducing liquefaction behaviour closer to the experimental results. A deeper investigation on many variables is expected for future studies after finalizing the model.

Acknowledgements

This work was supported by JSPS KAKENHI Grant Number JP20K20538. The authors acknowledge the financial support. In addition, we thank Takeshi Sato and Jirat Teparaksa who greatly assisted the research.

References

Adesina, P., O'Sullivan, C., Morimoto, T., Otsubo, M. "Determining a representative element volume for DEM simulations of samples with non-circular particles.", *Particuology,* 68, pp. 29-43, 2022. https://doi.org/10.1016/j.partic.2021.10.007

Al-Raoush, R., Alshibli, K.A. "Distribution of local void ratio in porous media systems from 3D X-ray microtomography images.", *Physica A: Statistical Mechanics and its Applications* 361, no. 2, pp. 441-456, 2006. https://doi.org/10.1016/j.physa.2005.05.043

Cundall, P.A., Strack, O.D. "A discrete numerical model for granular assemblies.", *geotechnique* 29, no. 1, pp. 47-65, 1979. https://doi.org/10.1680/geot.1979.29.1.47

Hertz, H.R. "Uber die Beruhrung fester elastischer Korper und Uber die Harte.", (On the contact of rigid elastic solids and on hardness), *Verhandlung des Vereins zur Beforderung des GewerbefleiBes, Berlin*, pp. 449, 1882. (in German)

Konishi, J., Naruse, F. "A note on fabric in terms of voids.", In *Studies in Applied Mechanics*, vol. 20, pp. 39-46. Elsevier, 1988. https://doi.org/10.1016/B978-0-444-70523-5.50012-6

Koseki, J., Yokoyama, D., Morimoto, T. "Cyclic bi-axial tests on assembly of metal rods under constant-volume condition to study re-liquefaction behavior.", *Transportation*

Infrastructure Geotechnology 7, no. 3, pp. 478-495, 2020. https://doi.org/10.1007/s40515-020-00123-w

Mindlin, R.D. "Compliance of elastic bodies in contact.", pp. 259-268, 1949. https://doi.org/10.1115/1.4009973

Mogami, T. "A statistical approach to the mechanics of granular materials.", *Soils and Foundations* 5, no. 2, pp. 26-36, 1965. https://doi.org/10.3208/SANDF1960.5.2_26

Morimoto, T., Otsubo, M., Koseki, J. "Microscopic investigation into liquefaction resistance of pre-sheared sand: Effects of particle shape and initial anisotropy.", *Soils and Foundations* 61, no. 2, pp. 335-351, 2021. https://doi.org/10.1016/J.SANDF.2020.12.008

Oda, M., Nemat-Nasser, S., Konishi, J. "Stress-induced anisotropy in granular masses.", *Soils and foundations* 25, no. 3, pp. 85-97, 1985. https://doi.org/10.3208/SANDF1972.25.3_85

Otsubo, M., Chitravel, S., Kuwano, R., Hanley, K. J., Kyokawa, H., Koseki, J. "Linking inherent anisotropy with liquefaction phenomena of granular materials by means of DEM analysis.", *Soils and Foundations* 62, no. 5, pp. 101202, 2022. https://doi.org/10.1016/J.SANDF.2022.101202

Plimpton, S. "Fast parallel algorithms for short-range molecular dynamics.", *Journal of computational physics* 117, no. 1, pp. 1-19, 1995. https://doi.org/10.1006/JCPH.1995.1039

Seed, H. B., Mori, K., Chan, C. K. "Influence of seismic history on liquefaction of sands.", *Journal of the Geotechnical Engineering Division* 103, no. 4, pp. 257-270, 1977. https://doi.org/10.1061/AJGEB6.0000399

Teparaksa, J., Koseki, J. "Effect of past history on liquefaction resistance of level ground in shaking table test.", *Géotechnique Letters* 8, no. 4, pp. 256-261, 2018. https://doi.org/10.1680/jgele.18.00085

Towhata, I. "Geotechnical Earthquake Engineering Springer.", *Berlin, Heidelberg*, 2008, https://doi.org/10.1007/978-3-540-35783-4

Wahyudi, S., Koseki, J., Sato, T. "Characteristics of re-liquefied behavior of sand by means of image analysis in stacked-rings shear apparatus.", *Bull Earthq Resist Struct Res Cent* 47, pp. 15-26, 2014.

Wakamatsu, K. "Recurrence of liquefaction at the same site induced by the 2011 Great East Japan Earthquake compared with previous earthquakes.", In *Proc. of the 15th World Conf. on Earthquake Engineering*, 2012.